BNL-22925

Recovery of T_c by Annealing of Irradiated A-15 Compounds

D. Dew-Hughes, S. Moehlecke and D. O. Welch

DISCLAIMER

Recovery of T_c by Annealing of Irradiated A-15 Compounds*

D. Dew-Hughes, S. Moehlecke+ and D. O. Welch
Brookhaven National Laboratory
Upton, New York 11973

Abstract

A model has been developed for the recovery of T_c in radiation-damaged A-15 compounds. This model has been applied to isothermal annealing data at 550°C on a sample of Nb_3Ge, and to isochronal annealing (200°C-900°C) data on V_3Si, Nb_3Ge and Nb_3Sn subjected to varying doses of fast neutrons, and on Nb_3Al of various compositions subjected to the same dose.

The recovery is assumed to take place by vacancy-assisted reordering and occurs in several stages. The major low-temperature stage involves a fairly stable population of irradiation-induced vacancies. At high temperatures these are replaced by thermal vacancies. Activation energies calculated for these processes, ~0.6-1.3 eV for site interchange, and ~1-2 eV for vacancy formation, are consistent with what is known about diffusion in the A-15 structure. Activation energies show some dependence upon radiation dose, but little upon composition.

---

*Work performed under the auspices of the U.S. Energy Research and Development Administration.
+On leave from Universidade Estadual de Campinas, Brazil, supported by Conselho Nacional de Pesquisas.

Introduction

The superconducting critical temperature T_c of compounds with the A-15 structure is particularly sensitive to radiation damage, and at sufficiently high doses can be reduced to a small saturation value. This loss of superconductivity is associated with radiation-induced disorder, and may be completely recovered by a suitable annealing treatment. Data is now being collected, either for isothermal or isochronal annealing, on the rate of recovery of T_c after irradiation, in a number of A-15 compounds.

The recovery of T_c is presumed to be a consequence of the re-ordering of the two species of atom on the A-15 lattice. One of us, (DOW) has accordingly developed a model for the kinetics of the reordering process in the A-15 structure. This model is based on Vineyard's theory for the reordering of AB bcc and AB_3 fcc alloys by a vacancy mechanism,[1] and the detailed derivation of the model will be given elsewhere.

The results of this model are applied to the experimental results of another of us (SM) on Nb_3Ge, Nb_3Al, and V_3Si, the details of which are to be found in a doctoral thesis[2]; and to the results of Karkin, et al. on Nb_3Sn.[3]

Theory

It is assumed that, in common with simpler metals, interstitials are mobile enough to anneal during an ambient temperature reactor

irradiation and, consequently, that reordering during subsequent annealing takes place by interchange of A atoms (Nb, V, etc.) on B sites with vacancies on A sites, and by B atoms (Al, Ga, Si, Ge, Sn, etc.) on A sites with vacancies on B sites. It is straightforward to apply Vineyard's theory of reordering by the vacancy mechanism[1] to the A-15 structure. Upon the assumption that, in the temperature range of interest, the equilibrium degree of order is very near unity and that the ordering energy is dominated by the A-A "covalent interaction" along the A-site chains, the model yields for the reordering kinetics:

$$\frac{d\zeta}{dt} = -f_v \frac{12\nu_A e^{-U_A/kT}\nu_B e^{-U_B/kT}}{\nu_B e^{-U_B/kT} + \frac{3}{4}\zeta\nu_A e^{-U_A/kT}} \zeta^2 \qquad (1)$$

where $\zeta \equiv (1-S)$, S being the usual Bragg-Williams order parameter, f_v is the fraction of vacant lattice sites, $\nu_A(\nu_B)$ is the attempt frequency and $U_A(U_B)$ the activation energy for the jump of an A (B) atom on a B (A) site into an adjacent vacancy on an A (B) site.

If the rate of jumping of an A atom into an A site is very much greater than the rate of jumping of a B atom into a B site, i.e. $\nu_A e^{-U_A/kT} >> \nu_B e^{-U_B/kT}$, then (1) becomes:

$$\frac{d\zeta}{dt} \cong -16\ f_v \nu_B e^{-U_B/kt}\zeta \qquad (2)$$

i.e. it is a first order process. If $\nu_B e^{-U_B/kT} >> \nu_A e^{-U_A/kT}$, or if ζ is small, then equation (1) becomes:

$$\frac{d\zeta}{dt} \cong -12\ f_v \nu_A e^{-U_A/kT} \zeta^2 \tag{3}$$

a second order process.

Integrating equations (2) and (3) yield, respectively:

$$\ell n\ \frac{\zeta}{\zeta_o} = 16\ f_v t \nu_B e^{-U_B/kT} \tag{4}$$

and

$$\frac{1}{\zeta} - \frac{1}{\zeta_o} = 12\ f_v t \nu_A e^{-U_A/kT} \quad . \tag{5}$$

If data from isothermal anneals are available, the order of the reordering process can be determined by whichever of $\ell n\zeta$ or $\frac{1}{\zeta}$ when plotted against time yields a straight line, provided that f_v is constant. Activation energies can be obtained from isochronal annealing data by plotting either $\ell n\ \ell n(\frac{\zeta_{i-1}}{\zeta_i})$ or $\ell n(\frac{1}{\zeta_i} - \frac{1}{\zeta_{i-1}})$ versus $\frac{1}{T_i}$, where ζ_i is the value at the end of the ith annealing step. Again it must be assumed that f_v does not change appreciably during each annealing step.

Unfortunately the experiments do not measure ζ, but the superconducting transition temperature, T_c. The value of T_c in irradiated samples does, however, seem to vary linearly with S provided $1>S>0.6$,[4] and in what follows ζ is taken as being proportional to $(1-\frac{T_c}{T_{co}})=y$, the experimentally determined quantity.

Results

Isothermal Anneals

There is only one extensive study of isothermal recovery of T_c, on a sample of Nb_3Ge, with an unirradiated T_c (T_{co}) of 20.29 K.[5] (This T_c value, and lattice parameter data, suggest the actual composition to be closer to $Nb_{76}Ge_{24}$.) After irradiation by fast neutrons to a dose of 2.6×10^{19} n/cm^2, the irradiated T_c was 4.21 K. The sample was annealed at 550°C, the annealing process being stopped at intervals for the measurement of T_c. In Fig. 1, both $\ell n \frac{y}{y_o}$ and $\frac{1}{y}$ are plotted versus t. Neither plot is particularly linear, but that of $\frac{1}{y}$ (second order) is marginally better. On this plot, the initial group of data points all lie below the straight line, and appear to approach it exponentially. This suggests that a proportion of the vacancies, f_{v_1} decay exponentially; the remaining fraction, f_{v_2}, staying essentially constant

$$\text{i.e.} \quad \frac{dy}{dt} = -\Gamma y^2 [f_{v_1} e^{-t/\tau} + f_{v_2}] \qquad (6)$$

which integrates to

$$\frac{1}{y} - \frac{1}{y_o} = \Gamma f_{v_2} t + \Gamma f_{v_1} \tau (1 - e^{-t/\tau}) \quad . \qquad (7)$$

From the slope of the line in Fig. 1, $\Gamma f_{v_2} \cong 0.0022$ min^{-1} and the intercept gives $\Gamma f_{v_1} \tau \cong 0.3$. The relaxation time, τ is, by inspection, ~25 minutes, and thus f_{v_1} represents about 85% of

vacancies initially present. A plot of $\frac{1}{y} - \frac{1}{y_o}$ versus $0.0022\ t + 0.3\ (1-e^{-t/25})$, Fig. 2, yields a very good straight line. The final point in Fig. 1, at 380 mins, and two further points at 1820 and 5660 mins, also fall below the line. This probably indicates that f_{v_2} is not really constant, but also decays exponentially, with a relaxation time which is ~10,000 min. This cannot be checked properly, as there are insufficient results at extremely long times.

The reordering process does, of itself, not result in a net loss of vacancies; these are merely exchanged between the two sublattices of the A-15 structure. The change in vacancy concentration can only be due to annihilation at sinks such as grain boundaries, dislocations, or other defects. The difference between the two fractions of vacancies can be either that those represented by f_{v_1} are spatially much closer to sinks than are those in f_{v_2}, or that there are some sinks which become saturated or exhausted after absorbing only f_{v_1} of the total vacancies. It is not possible to speculate further as to the exact nature of these sinks until something is known of the precise nature of radiation induced defects in the A-15 structure.

That the reordering process appears to be second order, even at relatively large values of ζ, is not particularly surprising. It implies that in the A-15 structure B atoms are more mobile than

A atoms. This is in line with what is known about growth of Nb_3Sn and V_3Ga in the solid state, which occurs by the diffusion of B atoms across the existing compound layer.[6]

Isochronal Anneals

The results of isochronal anneals on Nb_3Ge and Nb_3Sn irradiated to different doses, on 'Nb_3Al' of varying composition, and on V_3Si, are now analyzed. In view of the slight preference for a second order process displayed in the previous section, the analyses are presented in terms of a second order process. (In every case a first order analysis has also been carried out, and the results found to be worse than for the second order, although the conclusions reached are much the same.) From equation (5), it may be seen that the change in T_c during the i^{th} annealing step is given by

$$\frac{1}{Y_i} - \frac{1}{Y_{i-1}} \propto \nu_A e^{-U_A/kT_i} f_v(i) \qquad (8)$$

where $f_v(i)$ is the average vacanacy concentration during the i^{th} step. Thus the apparent activation energy for the recovery, Q, is:

$$Q \equiv -\frac{d\ell n\left(\frac{1}{Y_i}-\frac{1}{Y_{i-1}}\right)}{d(1/kT_i)} = U_A - \frac{d\ell n f_v(i)}{d(1/kT_i)} \quad . \qquad (9)$$

From the results of the previous section, there appears to be a fraction of the vacancy population which anneals out rapidly.

For annealing steps in which this process is occurring, $Q \cong U_A - E_m$, where E_m is the effective migration energy for the vacancy annealing. For annealing steps at higher temperatures during which the more stable vacancy population is annealing out slowly compared with the rate of reordering, $Q \cong U_A$. At still higher temperatures, where the radiation induced vacancies have annealed out, $Q \cong U_A + E_f$ where E_f is the vacancy formation energy.

$\underline{Nb_3Ge}$

Figure 3 shows the results of 2 hour isochronal anneals on three pieces of the same Nb_3Ge specimen subjected to the previously described isothermal anneal, each subjected to different doses of fast neutrons. In Fig. 4 $\ell n(\frac{1}{y_i} - \frac{1}{y_{i-1}})$ is plotted versus $1/T_i$, and four stages of reordering can be identified in the plot. Stage I, corresponding to the region of little change in T_c in Fig. 3, exists up to about 400°C and has a low slope. Stage II, between ~400-600°C, corresponds to 50-70% recovery of T_c and is reasonably linear on the Arrhenius plot. In Stage III, ~600-700°C, the rate of reordering appears to be constant or even decrease with increasing temperature, and at temperatures above ~700°C, the rate of reordering again increases with a slope greater than that of Stage II. The temperature range over which these various stages exist, and where appropriate the activation energies calculated therefrom, are given in Table I. A tentative interpretation of the results

is given in the discussion section.

$\underline{Nb_3Al}$

The results of 2 hour isochronal anneals for four samples of 'Nb_3Al' of different composition, irradiated to approximately the same dose of fast neutrons, are shown in Fig. 5. Up to ~525°C, the recovery process appears to be independent of composition. Above 525°C the different compositions recover at different rates; the greater the departure from stoichiometry the slower the rate of recovery. Above 800°C a drop in T_c is seen for those samples with excess niobium. This is associated with precipitation of the bcc solid solution phase.

Figure 6 is a plot of $\ell n(\frac{1}{Y_i} - \frac{1}{Y_{i-1}})$ vs $\frac{1}{T_i}$. This differs a little from that of Nb_3Ge, in that Stage II shows two slopes. Stage IIa, corresponding to the region of recovery independent of composition, has a much lower slope than that of Stage IIb above 525°C. Within the scatter of the points, the slopes are independent of composition. Again the results are listed in Table I.

$\underline{V_3Si}$

The results of 2 hour isochronal anneals for one sample of V_3Si is shown in Fig. 7. Differences in comparison with the previous samples are that (i) recovery begins at much lower temperatures (250°C versus 450°C), (ii) there is a very rapid increase in T_c between 400 and 450°C, and (iii) after the rate of

T_c increase appears to tail-off at ~500°C, it then shows a faster rate above 650°C and almost total recovery of T_{co} at 700°C.

These differences become even more apparent in the plot of $\ell n(\frac{1}{y_i} - \frac{1}{y_{i-1}})$ versus $\frac{1}{T}$, Fig. 8. Stage II has a very low slope, Stage III is separated from Stage II by a large jump, and Stage IV has an extremely high slope. More data, including different irradiation dosages, and isothermal annealing curves, are necessary on this material before a proper comparison can be made with the other A-15 compounds.

$\underline{Nb_3Sn}$

There are, as yet, few reports of annealing studies on irradiated A-15 compounds in the literature. A reasonably detailed isochronal study on Nb_3Sn was carried out by Karkin et al.[3] Specimens were annealed for 20 minutes at each temperature, following one of three doses of fast neutrons. The rate of T_c recovery increases with increasing temperature up to the point of almost complete restoration of the original T_c. The curves are not sigmoidal as found in this work.

Their results are analyzed in terms of the above model in Fig. 9. In comparison with previous results there appears to be no Stage III in the process. The data is insufficient also to determine the true existence of a linear Stage IV. The activation energies quoted for Stage IV must be regarded as tentative.

Discussion

The results are summarized in Table I. Stage I, where it occurs, is thought to be associated with the initially high fraction of mobile vacancies, f_{v_1}, which are annihilated in the early portion of the annealing process.

Stage II represents the reordering of displaced atoms by means of a longer lived fraction of radiation induced vacancies, f_{v_2}. The activation energy for this process increases with increasing fast neutron dose. It is not at all clear why there should be two activation energies for the Nb_3Al specimens. The Stage II activation energies, U, are plotted versus R_A/R_B, the radius ratio of the A and B atoms, according to the modified Geller scheme,[7] in Fig. 10. It would seem that U is linearly proportional to R_A/R_B, the slope increasing for increasing radiation dose. It is interesting to note that extrapolation of these points cuts the U=0 axis at $R_A/R_B \cong 0.94$. This is the most probable value of R_A/R_B as found by Hartsough[8] for the A-15 structure. The significance, if any, of this result is not at present understood. The trend is contradictory to that found by Luhman and Sweedler.[9] This plot predicts for V_3Ga a value of U=0.025 eV. If correct, this would explain the difficulty experienced in trying to disorder V_3Ga by irradiation at reactor temperature (~140-200°C).[2]

Stage II is thought to end with the exhaustion of the radiation induced vacancies, i.e., $fv_2 \rightarrow 0$, at the usual vacancy sinks. Stage III is an intermediate regime between Stages II and IV, and is absent if II and IV overlap. Stage IV, which represents an increase in the rate of recovery of T_c, is in a temperature range in which the generation of thermal vacancies is likely to be significant. Reordering now takes place with the aid of thermal vacancies; the measured activation energy is U plus the energy of formation of an A-site vacancy. The difference between Stage II and Stage IV energies is this vacancy formation energy. Values of ~1.4 eV for Nb_3Ge, 1.1 eV for Nb_3Al, 1.2-2.2 eV for Nb_3Sn seem entirely reasonable. The value, ~5.8 eV, for V_3Si, is much too large.

Taking an average value for the formation energy of vacancies in the A-15 structure of ~1.5 eV and subtracting this from "typical" activation energies for self-diffusion of tin through Nb_3Sn[10] and gallium through V_3Ga,[11] ~2.5-2.8 eV, estimated from rates of layer growth, suggests that the migration energy of vacancies is of the order of 1 eV, comparable to the activation energies in Stage II recovery of order. Though the processes of layer growth involve the movement of B atoms on the B sublattice, and are therefore not identical with the reordering processes studied here, the consistency of the results is satisfying.

Conclusions

1. The recovery of T_c in A-15 compounds upon annealing after irradiation has been interpreted as being due to a vacancy-assisted reordering process.

2. A model for the reordering process has been developed, based upon Vineyard's theory. The process follows second order kinetics.

3. The reordering process is characterized by a first stage during which the initial vacancy population is rapidly reduced, a second stage in which reordering is assisted by a fairly stable population of radiation-induced vacancies, a transition stage during which the radiation-induced vacancies are depleted, and a final stage involving thermal vacancies.

This analysis has pointed out the need for more detailed results on the recovery of irradiated A-15 superconductors. More materials should be studied, in which composition, dose and type of ionizing radiation are varied. Irradiations carried out at ~20 K are necessary to characterize the types of defects produced in these structures. Long-time isothermal anneals are necessary to properly determine the order of the kinetics of the recovery processes. It is hoped that this paper will stimulate further efforts in these areas.

References

1. G. H. Vineyard, Phys. Rev. 102, 981 (1956).
2. S. Moehlecke, Ph.D. Thesis, Campinas (1977).
3. A. E. Karkin, V. E. Arknikov, B. N. Goshchitsky, E. P. Romanov and S. K. Sidorov, Phys. Stat. Sol. (a)38, 433 (1976).
4. A. R. Sweedler, private communication.
5. A. R. Sweedler, D. E. Cox, S. Moehlecke, R. H. Jones, L. R. Newkirk and F. A. Valencia, J. Low Temp. Phys. 24, 645 (1976).
6. H. H. Farrell, G. H. Gilmer and M. Suenaga, Thin Solid Films, 25, 253 (1975).
7. G. R. Johnson and D. H. Douglass, J. Low Temp. Phys. 14, 656 (1974).
8. L. D. Hartsough, J. Phys. Chem. Solids 35, 1691 (1974).
9. T. S. Luhman and A. R. Sweedler, Phys. Lett. 58A, 355 (1976).
10. R. Nunez-Doval, M.S. Thesis, University of Texas, Austin (1974).
11. D. Dew-Hughes, to be published.

Table I

Specimen	T_{co}(K)	Dose (n/cm^2)	T_{c_i}(K)	Stage I Temp.(°C)	Stage II Temp.(°C)	Stage II ΔG(eV)	Stage III Temp.(°C)	Stage IV Temp.(°C)	Stage IV ΔG(eV)
		$7x10^{18}$	12.28	300-425	425-575	0.9	575-625	625-725	2.3
b_3Ge	20.29	$2.6x10^{19}$	4.15	" "	425-600	1.0	600-700	700-800	-
		$5x10^{19}$	3.35	" "	425-675	1.3	675-750	-	-
$b_{74}Al_{26}$	18.50	$5x10^{19}$	3.57	-	350-450 (a)	0.6 (a)			
$b_{76.8}Al_{23.2}$	18.29	$4.7x10^{19}$	3.80	300-350			550-650	650-750	2.2
$b_{79.8}Al_{20.2}$	13.10	$4.7x10^{19}$	4.10	300-350	450-550 (b)	1.1 (b)			
$b_{81.3}Al_{18.7}$	10.23	$4.7x10^{19}$	4.40	300-350					
$_3Si$	16.70	$2.6x10^{19}$	3.41	?	300-400	0.25	450-625	650-700	6.1
		$2x10^{19}$	11.5			0.6			1.8
b_3Sn	17.7	$6x10^{19}$	5.5	-	300-700	0.7	—	700-1000	2.9
		$7x10^{19}$	2.8			0.7			2.9

Figure Captions

Fig. 1. $\ell n\frac{y}{y_o}$, and $\frac{1}{y}$, plotted versus annealing time, for a sample of Nb_3Ge annealed at 550°C.

Fig. 2. $\frac{1}{y} - \frac{1}{y_o}$ plotted versus a function of annealing time $t[=0.0022t+0.3(1-e^{-t/25})]$, for the sample of Nb_3Ge shown in Fig. 1.

Fig. 3. 2 hour isochronal annealing curves for Nb_3Ge after irradiation to three different doses of fast neutrons.

Fig. 4. $\ell n(\frac{1}{y_i}-\frac{1}{y_{i-1}})$ versus $\frac{1}{T}$ for the Nb_3Ge samples shown in Fig. 3.

Fig. 5. 2 hour isochronal annealing curves for samples of Nb_3Al of differing compositions, after irradiation to the same dose of fast neutrons.

Fig. 6. $\ell n(\frac{1}{y_i}-\frac{1}{y_{i-1}})$ versus $\frac{1}{T}$ for the Nb_3Al samples shown in Fig. 5.

Fig. 7. 2 hour isochronal annealing curve for a sample of V_3Si after fast neutron irradiation.

Fig. 8. $\ell n(\frac{1}{y_i}-\frac{1}{y_{i-1}})$ versus $\frac{1}{T}$ for the V_3Si sample shown in Fig. 5.

Fig. 9. $\ell n(\frac{1}{y_i}-\frac{1}{y_{i-1}})$ versus $\frac{1}{T}$ for samples of Nb_3Sn after irradiation to three different doses of fast neutrons, data from reference (3).

Fig. 10. Activation energy for Stage II of isochronal recovery, plotted versus the Geller radius ratio, R_A/R_B, for several A-15 samples.

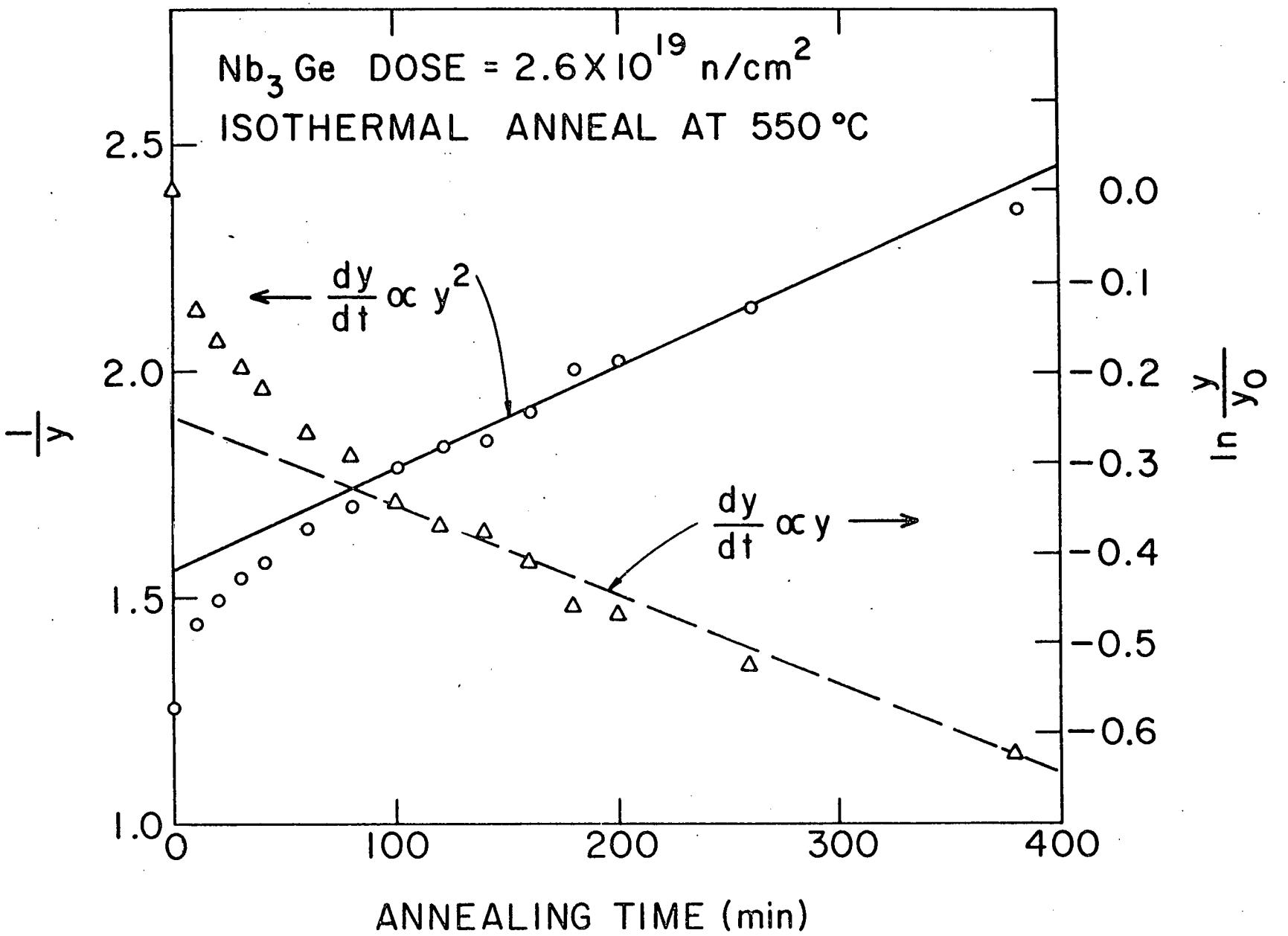
Nb_3Ge DOSE = 2.6×10^{19} n/cm^2
ISOTHERMAL ANNEAL AT 550 °C
$\frac{dy}{dt} \propto y^2$
$\frac{dy}{dt} \propto y$
$-\frac{1}{y}$
$\ln \frac{y}{y_0}$
2.5
2.0
1.5
1.0
0.0
−0.1
−0.2
−0.3
−0.4
−0.5
−0.6
0
100
200
300
400
ANNEALING TIME (min)

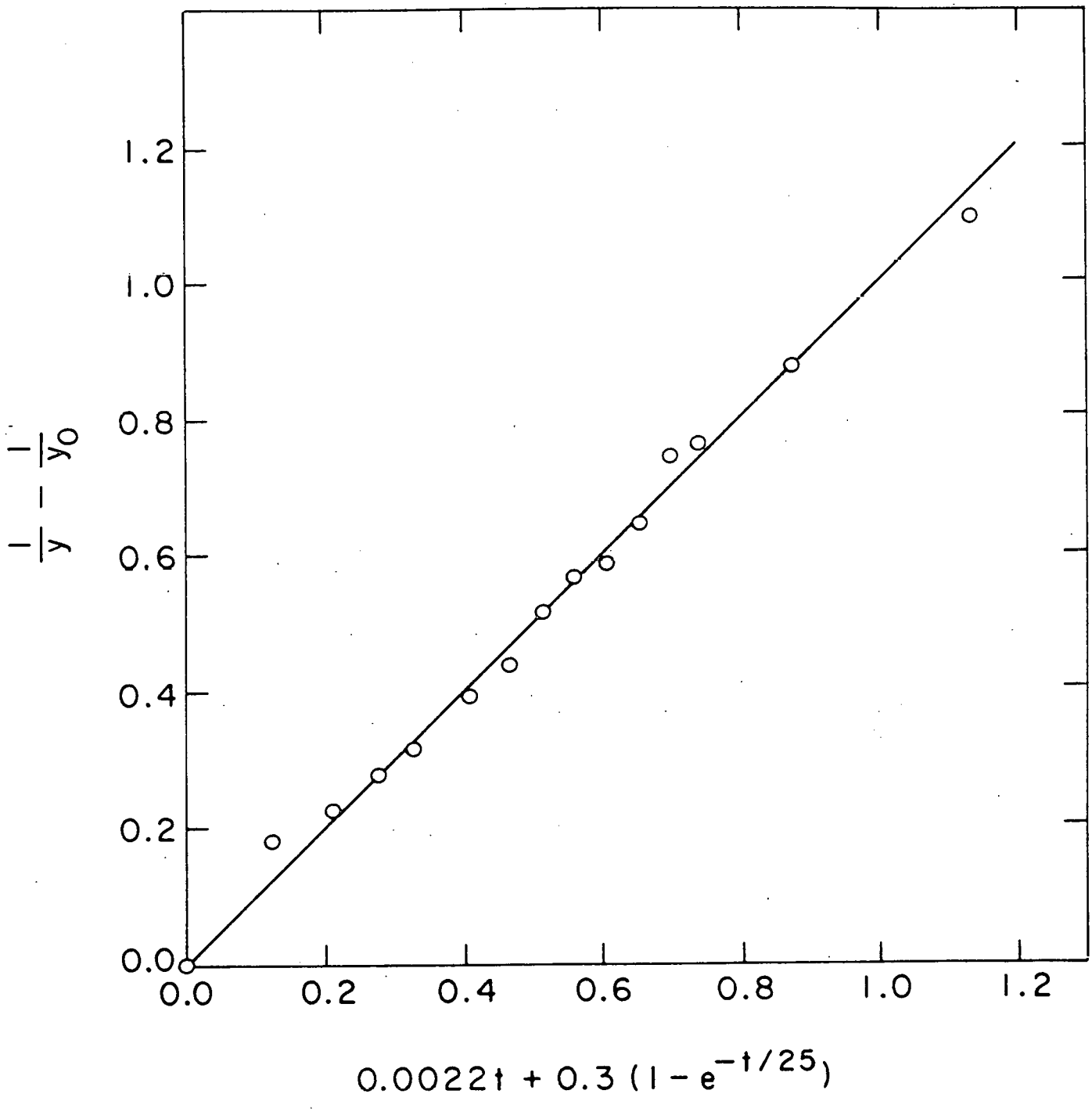
1.2
1.0
0.8
0.6
0.4
0.2
0.0
0.0
0.2
0.4
0.6
0.8
1.0
1.2
$\frac{1}{y} - \frac{1}{y_0}$
$0.0022t + 0.3\,(1 - e^{-t/25})$

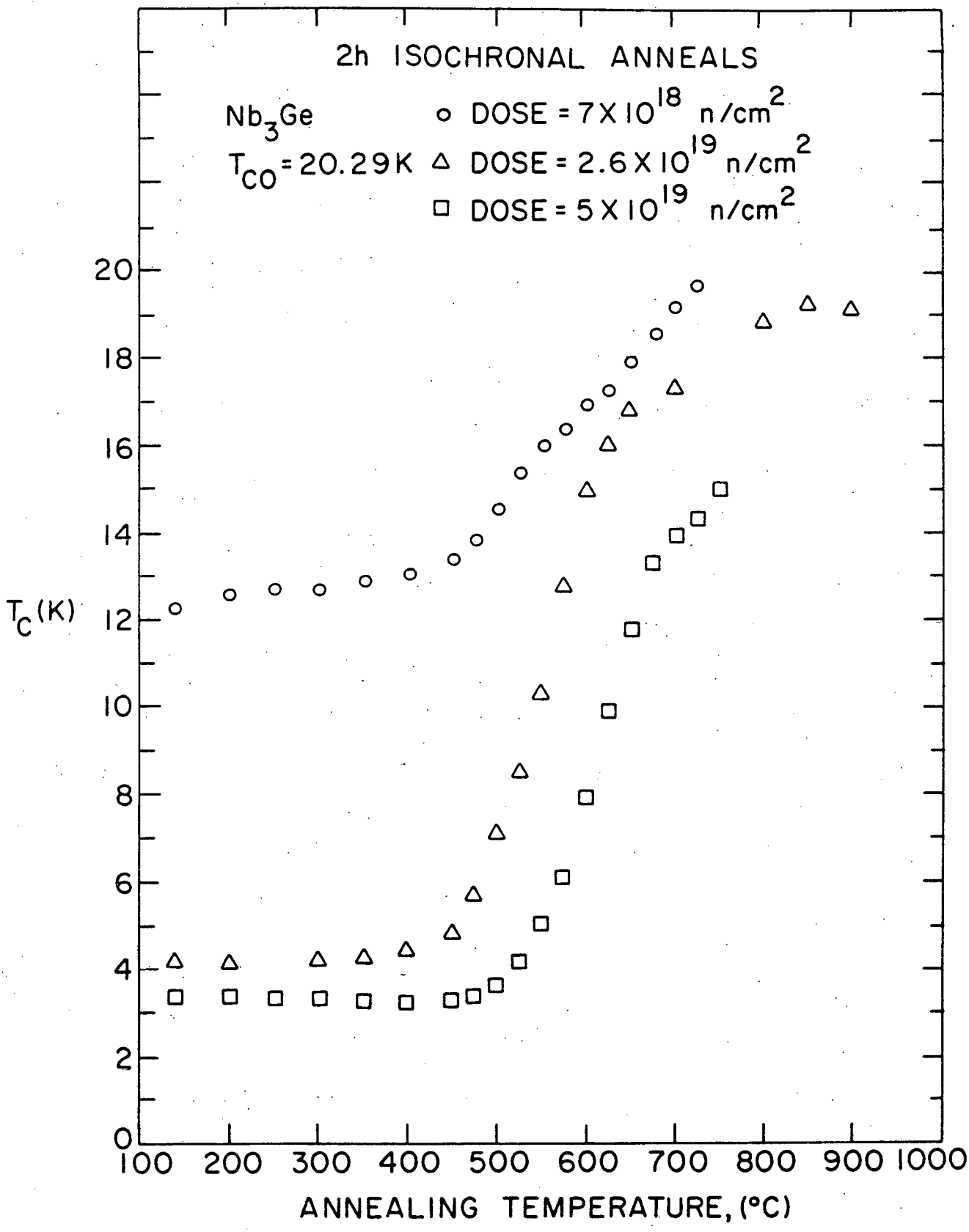
2h ISOCHRONAL ANNEALS
Nb3Ge
TCO = 20.29K
o DOSE = 7X10^18 n/cm^2
Δ DOSE = 2.6X10^19 n/cm^2
□ DOSE = 5X10^19 n/cm^2
TC(K)
0
2
4
6
8
10
12
14
16
18
20
100
200
300
400
500
600
700
800
900
1000
ANNEALING TEMPERATURE, (°C)

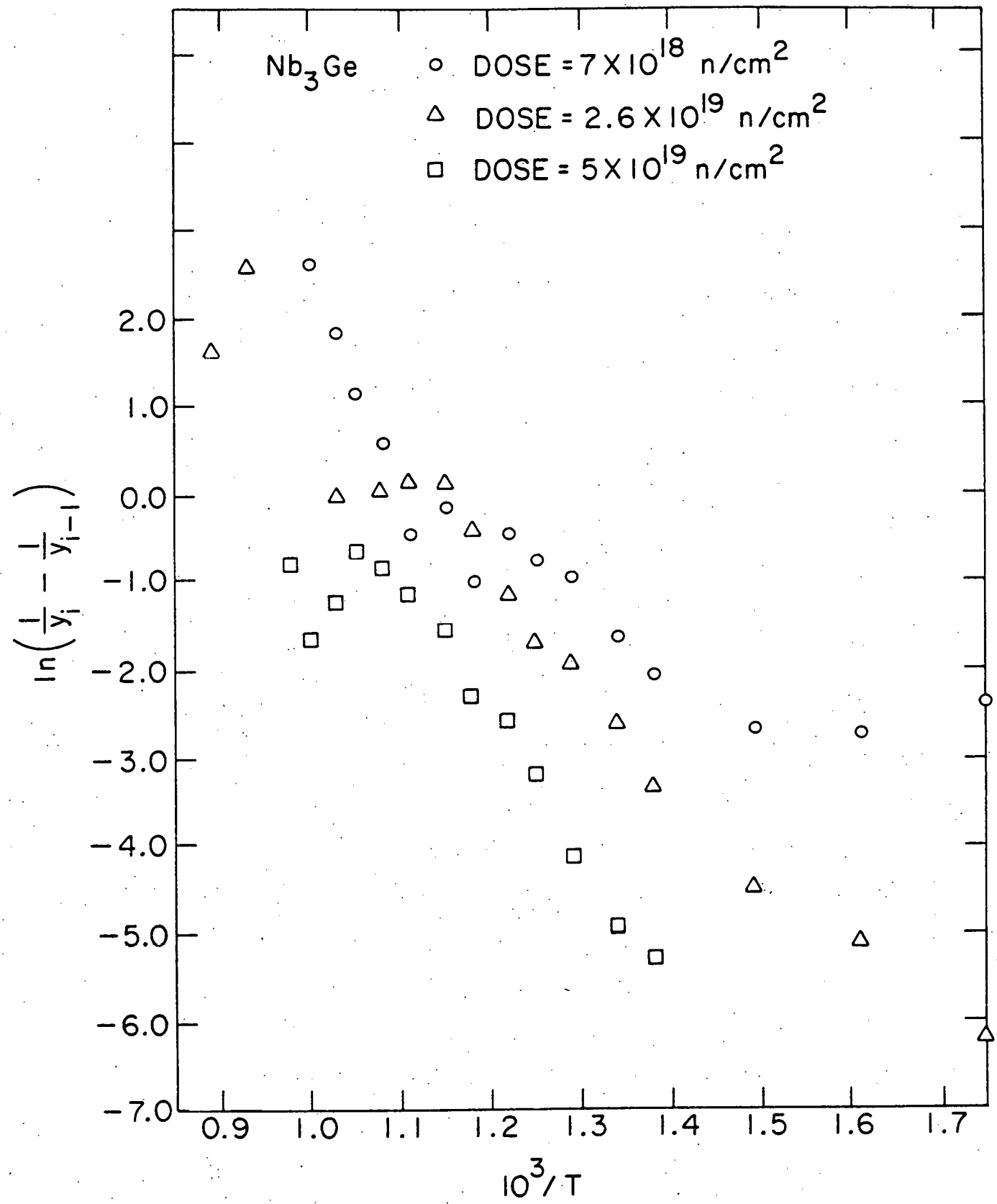
Nb3Ge
DOSE = 7 X 10^18 n/cm^2
DOSE = 2.6 X 10^19 n/cm^2
DOSE = 5 X 10^19 n/cm^2
2.0
1.0
0.0
-1.0
-2.0
-3.0
-4.0
-5.0
-6.0
-7.0
0.9
1.0
1.1
1.2
1.3
1.4
1.5
1.6
1.7
10^3/T
ln(-1/y_i - -1/y_i-1)

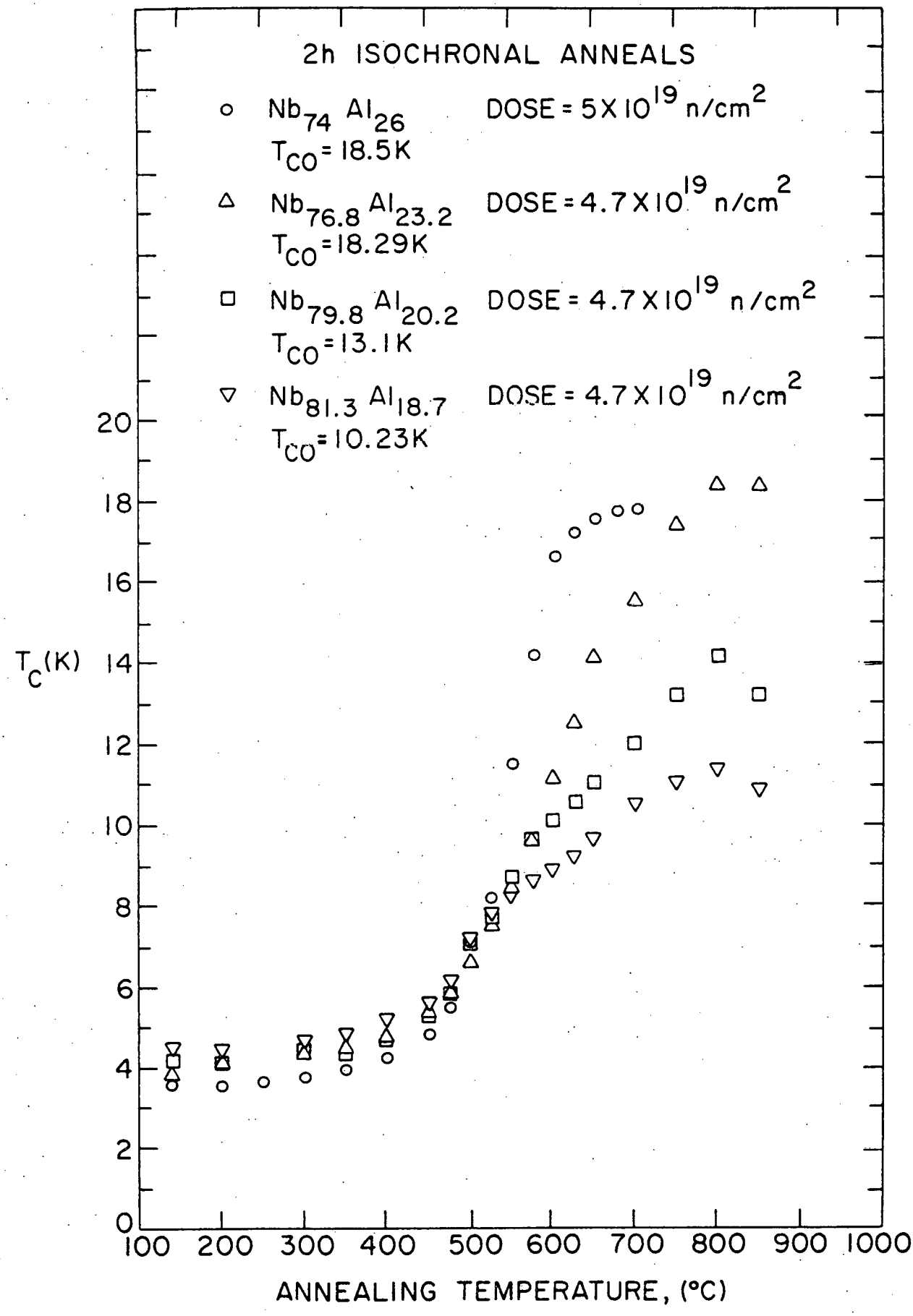
2h ISOCHRONAL ANNEALS
Nb74 Al26
TCO = 18.5K
DOSE = 5X10^19 n/cm^2
Nb76.8 Al23.2
TCO = 18.29K
DOSE = 4.7X10^19 n/cm^2
Nb79.8 Al20.2
TCO = 13.1K
DOSE = 4.7X10^19 n/cm^2
Nb81.3 Al18.7
TCO = 10.23K
DOSE = 4.7X10^19 n/cm^2
TC(K)
0
2
4
6
8
10
12
14
16
18
20
100
200
300
400
500
600
700
800
900
1000
ANNEALING TEMPERATURE, (°C)

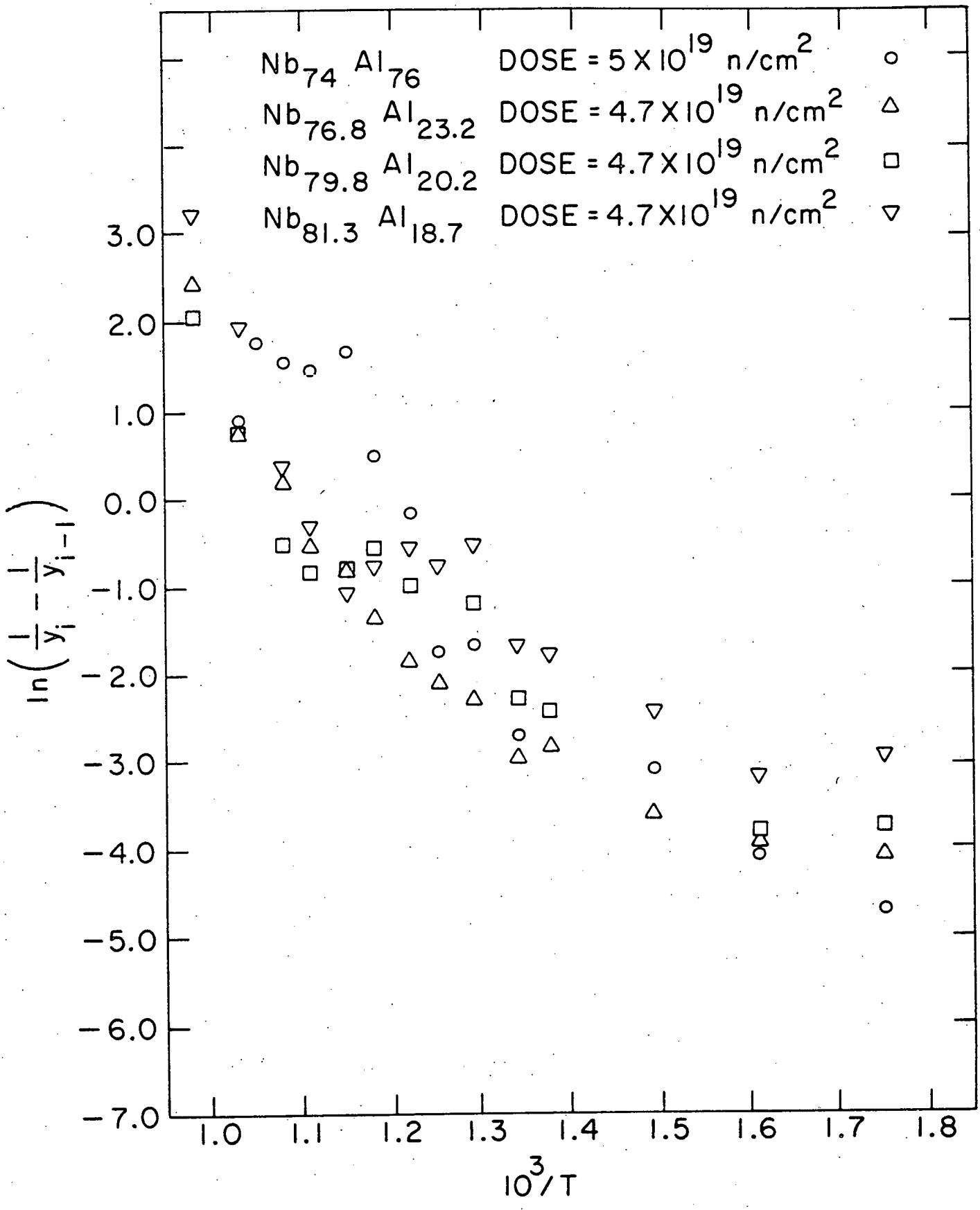
$Nb_{74}\ Al_{76}$ DOSE = 5×10^{19} n/cm^2
$Nb_{76.8}\ Al_{23.2}$ DOSE = 4.7×10^{19} n/cm^2
$Nb_{79.8}\ Al_{20.2}$ DOSE = 4.7×10^{19} n/cm^2
$Nb_{81.3}\ Al_{18.7}$ DOSE = 4.7×10^{19} n/cm^2
$\ln\left(\frac{-\frac{1}{y_i} - \frac{1}{y_{i-1}}}{-\frac{1}{y_i}}\right)$
3.0
2.0
1.0
0.0
−1.0
−2.0
−3.0
−4.0
−5.0
−6.0
−7.0
1.0
1.1
1.2
1.3
1.4
1.5
1.6
1.7
1.8
$10^3/T$

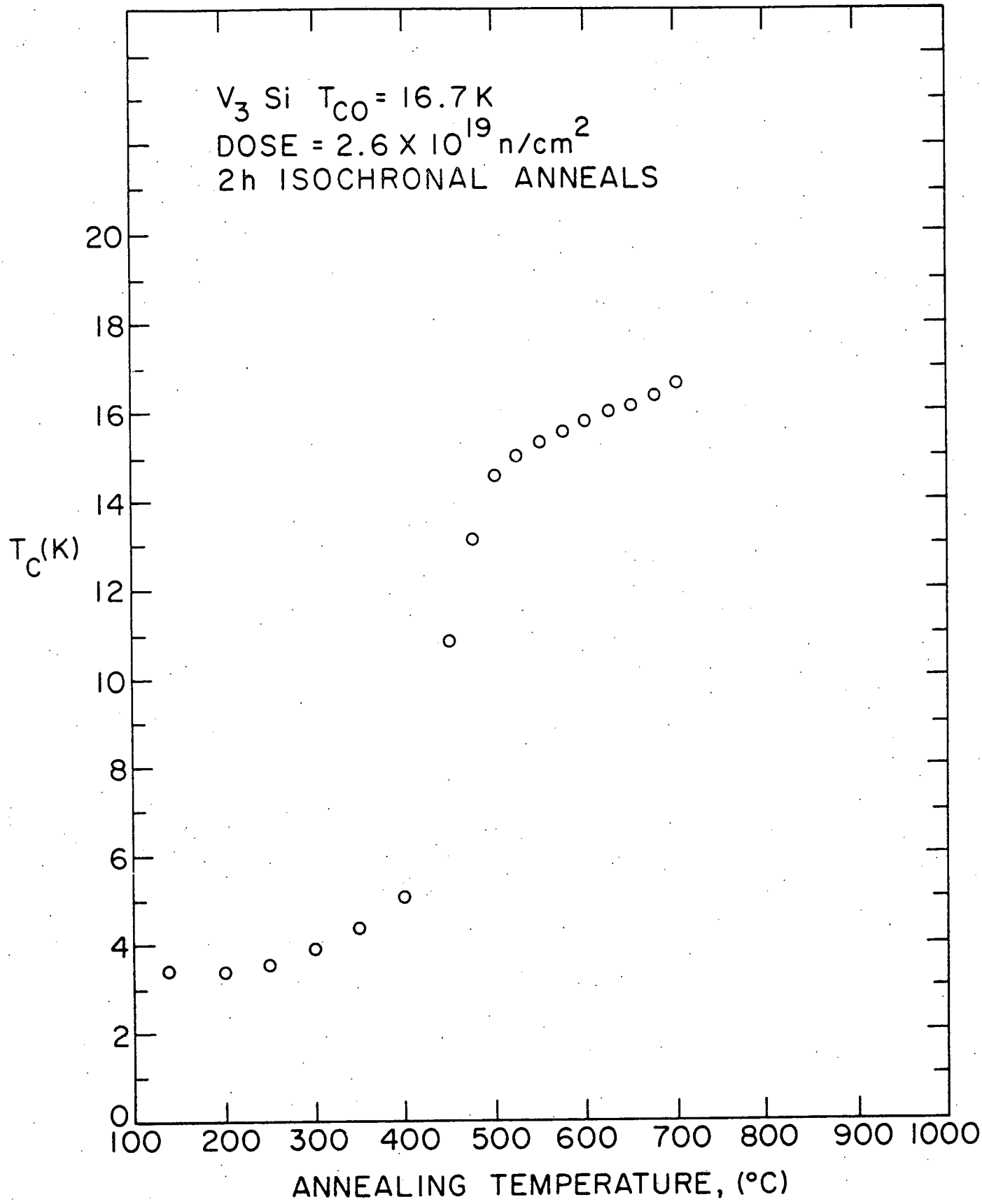
V_3 Si T_{CO} = 16.7 K
DOSE = 2.6 X 10^{19} n/cm^2
2h ISOCHRONAL ANNEALS
T_C(K)
0
2
4
6
8
10
12
14
16
18
20
100
200
300
400
500
600
700
800
900
1000
ANNEALING TEMPERATURE, (°C)

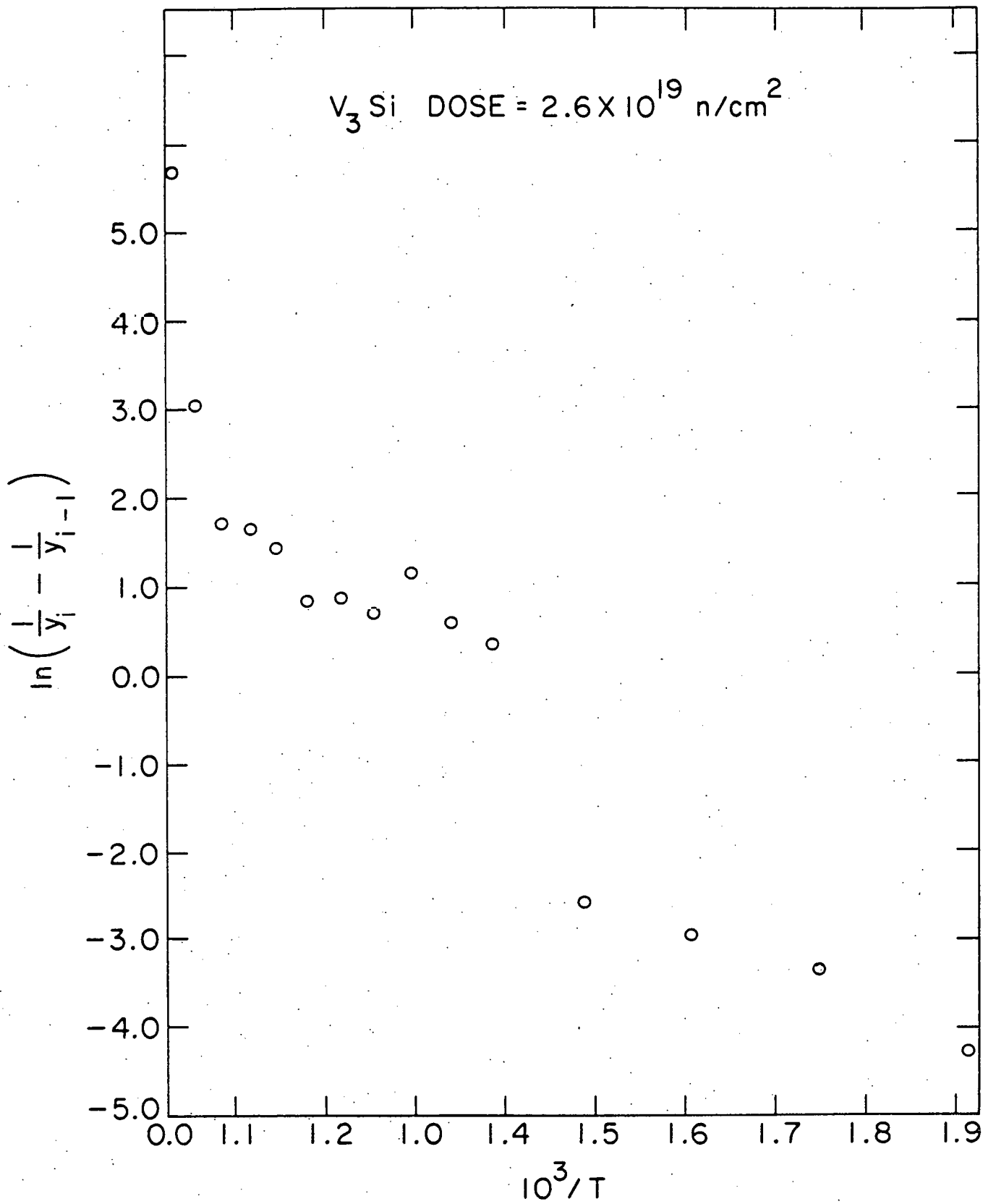
V_3Si DOSE = 2.6×10^{19} n/cm^2
$\ln\left(\frac{-\frac{1}{y_i} - \frac{1}{y_{i-1}}}{-\frac{1}{y_i}}\right)$
5.0
4.0
3.0
2.0
1.0
0.0
-1.0
-2.0
-3.0
-4.0
-5.0
0.0
1.1
1.2
1.0
1.4
1.5
1.6
1.7
1.8
1.9
$10^3/T$

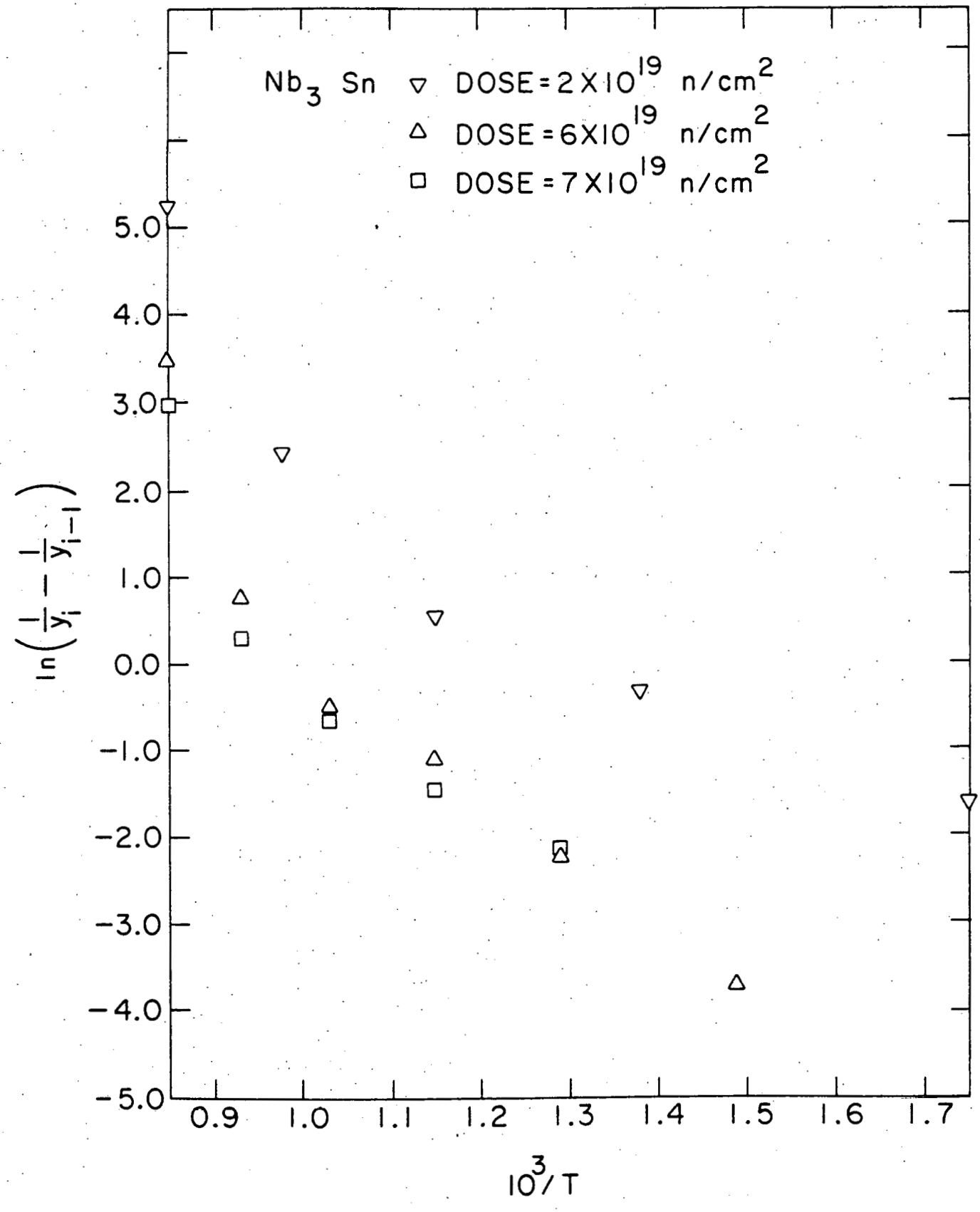
Nb3 Sn
DOSE = 2X10^19 n/cm^2
DOSE = 6X10^19 n/cm^2
DOSE = 7X10^19 n/cm^2
5.0
4.0
3.0
2.0
1.0
0.0
-1.0
-2.0
-3.0
-4.0
-5.0
0.9
1.0
1.1
1.2
1.3
1.4
1.5
1.6
1.7
10^3/T
ln (1/y_i - 1/y_i-1)

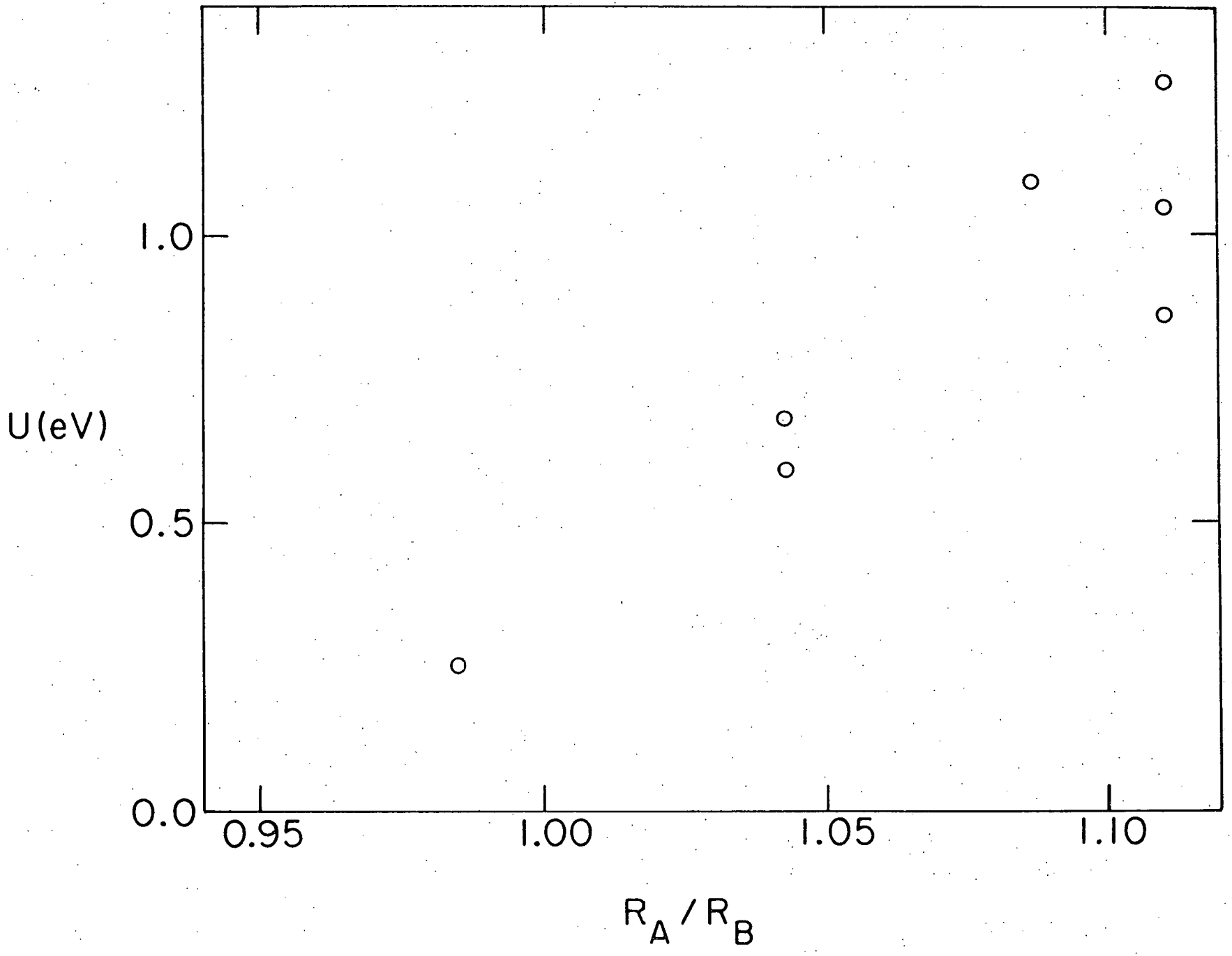
1.0
0.5
0.0
U(eV)
0.95
1.00
1.05
1.10
R_A / R_B